Supramolecular Chemistry: Molecular Recognition and Self-Assembly Using Rigid Spacer-Chelators Bearing Cofacial Terpyridyl Palladium(II) Complexes Separated by 7 Å

Roger D. Sommer,[†] Arnold L. Rheingold,*[,†] Andrew J. Goshe,[‡] and B. Bosnich*[,‡]

Contribution from the Department of Chemistry and Biochemistry, University of Delaware, Newark, Delaware 19716, and Department of Chemistry, The University of Chicago, 5735 S. Ellis Ave., Chicago, Illinois 60637

Received December 18, 2000

Abstract: Partially and fully aromatic molecular spacers bearing two symmetrically bound terpyridyl chelators have been prepared. These spacer-chelators were constructed to dispose the two terpyridyl ligands and their complexes with square planar metals cofacially with a separation of about 7 Å between the two metals. Dipalladium(II) complexes of these spacer-chelators were prepared and characterized. These palladium complexes readily form large molecular rectangles with a linear linker such as 4,4′-dipyridyl. The dichlorodipalladium complex of the partially reduced spacer-chelator is capable of incarcerating planar aromatic and coordination compounds as guests. A crystal structure showing the incorporation of 9-methylanthracene has been determined. A 9-methylanthracene lies completely within the ∼7 Å space provided by the cleft formed by the two cofacially disposed chloro−palladium−terpyridyl units. The crystal structure shows additional π-stacking interactions between a second 9-methylanthracene and neighboring receptors.

Introduction

Inspired by biology and driven by applications in materials science, supramolecular chemistry has witnessed some remarkable recent achievements.[1] Although much of the early work relied on purely organic structures derived from kinetically formed strong bonds, more recent endeavors have been directed at thermodynamically controlled self-assembly using weak interactions, principally hydrogen bonds.[2] Once formed, many of these structures, whether kinetically or thermodynamically formed, can incarcerate molecules through electrostatic[3] and dispersion forces.[4] During the development of these purely organic systems, it became apparent that transition metal complexes possessing kinetically labile but thermodynamically stable coordinate bonds provided ready entry into large, highly charged, complex structures. Like their organic counterparts, these also are capable of molecular recognition by incarceration of molecules in the cavities provided by the receptor. Because of the ready variation of charge, potential weak interactions of the metals with the guest, the unique valence directionalities of transition metals, thermodynamic control of assembly, and metal redox behavior, transition metal-based supramolecular structures provide special characteristics which are not readily available to purely organic systems.

Three basic approaches have been adopted when labile transition metals are used to prepare supramolecular assemblies. One method, the unrestricted metal-linker approach, is to mix a transition metal salt with a linker ligand and to allow the product to crystallize.[5] In this way, large, complex, crystalline arrays can be generated, the structures of which depend on the valence geometry of the metal, the shape of the linking ligand, the counterion, and solubility. This form of crystal engineering can lead to oligomeric or polymeric structures, some of which, in the absence of lattice interpenetration, are capable of occluding molecules in the molecular cavities. Whereas fascinating mesoscopic structures can be produced in this way, the method suffers from an absence of a set of guiding principles, which might predict structure.

Another approach, the polynuclear ligand method, involves the synthesis of polybidentate or sometimes polytridentate ligands that can bind several metals in sequence. Such ligands can, for example, provide oligonuclear helicates and grids.[6,7] Similarly, bidentate ligands supported by spacers can provide

[†] University of Delaware.

[‡] The University of Chicago.

(1) (a) Leininger, S.; Olenyuk, B.; Stang, P. J. *Chem. Rev.* **2000**, *100*, 853−908. (b) Swiegers, G. F.; Malefetse, T. J. *Chem. Rev.* **2000**, *100*, 3483−3537. (c) Jones, C. J. *Chem. Soc. Rev.* **1998**, *27*, 289−299. (d) Biradha, K.; Fujita, M. *Advances in Supramolecular Chemistry*; Gokel, G. W., Ed.; JAI Press Inc.: Stamford, CT, 2000; pp 1−39. (e) *Comprehensive Supramolecular Chemistry*; Lehn, J.-M., Chair Ed.; Atwood, J. L., Davis, J. E. D., MacNicol, D. D., Vögtle, F., Exec. Eds.; Permagon: Oxford, UK, 1996; Vol. 1−11.

(2) (a) Rudkevich, D. M.; Rebek, J., Jr. *Eur. J. Org. Chem.* **1999**, *1991*, 1−2005. (b) Rebek, J., Jr. *Pure Appl. Chem.* **1996**, *68*, 1261−1266. (c) Conn, M. M.; Rebek, J., Jr. *Chem. Rev.* **1997**, *97*, 1647−1668. (d) Weber, E. *Design of Organic Solids*; Springer: Berlin, 1998; pp 97−127. (e) Chang, S. K.; Hamilton, A. D. *J. Am. Chem. Soc.* **1988**, *110*, 1318−1319. (f) Whitesides, G. M.; Simanek, E. E.; Mathias, J. P.; Seto, C. T.; Chin, D. N.; Mammen, M.; Gordon, D. M. *Acc. Chem. Res.* **1994**, *28*, 37−44.

(3) (a) Schneider, H.-J.; Schiestel, T.; Zimmerman, P. *J. Am. Chem. Soc.* **1992**, *114*, 7698−7703. (b) Schmidtchen, F. P. *Angew. Chem., Int. Ed.* **1977**, *10*, 720−721. (c) Kearney, P. C.; Mizoue, L. S.; Kumpf, R. A.; Forman, J. E.; McCurdy, A.; Dougherty, D. A. *J. Am. Chem. Soc.* **1993**, *115*, 9907−9919.

(4) (a) Hunter, C. A.; Sanders, J. K. M. *J. Am. Chem. Soc.* **1990**, *112*, 5525−5534.

(5) (a) Hagrman, P. J.; Hagrman, D.; Zubieta, J. *Angew. Chem., Int. Ed.* **1999**, *38*, 2638−2684. (b) Blake, A. J.; Champness, N. R.; Hubberstey, P.; Li, W.-S.; Withersby, M. A.; Schröder, M. *Coord. Chem. Rev.* **1999**, *138*, 117−138.

(6) (a) Hasenknopf, B.; Lehn, J.-M.; Boumediene, N.; Dupont-Gervais, A.; Van Dorsselaer, A.; Kneisel, B.; Fenske, D. *J. Am. Chem. Soc.* **1997**, *119*, 10956−10962. (b) Hasenknopf, B.; Lehn, J.-M.; Boumediene, N.; Leize, E.; Van Dorsselaer, A. *Angew. Chem., Int. Ed.* **1998**, *37*, 3265−3268.

10.1021/ja004279v CCC: $20.00
Published on Web 04/05/2001

macrocyclic polyhedra.[8−10] In all of these cases, the shape and size of the supramolecular structure is controlled by the denticity of the ligands, their spacer components, and the coordination characteristics of the metal. In some cases, these structures provide cavities for substrate incarceration, but in most cases it is the appealing nature of the structures that has been pursued.

Unlike the unrestricted metal-linker method, but resembling the polynuclear ligand approach, the third method relies on constraining the number and geometry of the metal coordination sites combined with a particular linker ligand geometry and denticity in order to obtain supramolecular structures of a specific size and topology. This approach has been developed

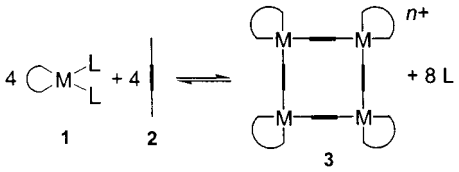

by Fujita[11] and Stang[12] and has proved to be remarkably successful in that predictable supramolecular structures are formed in essentially quantitative yield under thermodynamic control. In essence the Fujita method employs a square planar complex of Pd^{2+} or Pt^{2+} bearing an inert bidentate ligand with easily displaced ligands, L, in the remaining cis-disposed coordination sites, **1**. If a linear linker, **2**, such as 4,4′-dipyridyl is used, a quantitative yield of the square, **3**, is slowly formed.[13] In a similar way by using, **1**, and the tripyridyl linker, **4**, the three-dimensional triangular structure, **5**, is isolated.[14]

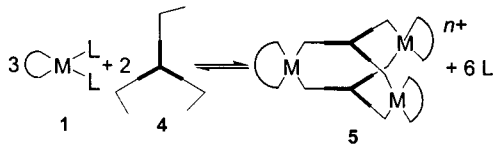

By the use of, **1**, and a variety of linkers, complex but symmetrical structures are readily formed, approaching and some achieving the nanoscale. Many of the larger structures have been shown to incarcerate multiple guest molecules.[11] A variation of this approach employs octahedral complexes where three of the vicinal coordination positions carry a kinetically inert tridentate ligand, **6**. Addition of linear ligand linker, **2**, to, **6**, results in the formation of the cube structure, **7**.[15] These systems have not, as yet, been developed as much as those derived from, **1**. In all of these cases, both with square planar and octahedral complexes, the size of the supramolecular structures is determined largely by the dimensions of the linker, and the metals serve as connections at the apexes of the molecular array.

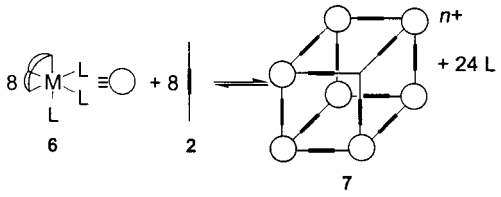

We describe here a somewhat different approach to the formation of inorganic supramolecular structures under thermodynamic control. In some respects, the idea borrows elements from the polynuclear ligand method and the constrained metal valency approach just described. Square planar d^8 transition metal complexes formed from planar aromatic ligands are known to form stacked crystal structures which have weak metal−metal bonding and attractive $\pi-\pi$-stacking.[16] These stabilizing interactions are sometimes observed in concentrated solutions.[16] One consequence of these conglomerates is the appearance of new electronic spectroscopic features which have been the subject of numerous studies.[16] The metal−metal separations are about 3.5 Å which is similar to the separation between π-stacked aromatic molecules.[4] Consequently, to provide a receptor for square planar d^8 complexes with planar aromatic ligands and also purely organic aromatic molecules, a spacer-chelator molecule is required which holds the chelators cofacially at a separation of about 7 Å. The elements of such a structure are illustrated in, **8**, which shows two cofacial tridentate chelators bound to a square planar metal.

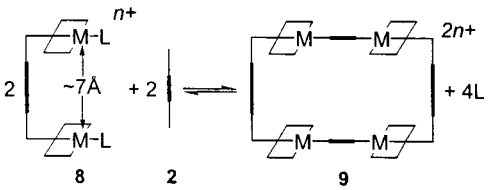

Provided the unidentate ligand, L, in **8**, is a good leaving group, addition of a linear linker, **2**, such as 4,4′-dipyridyl, should generate the molecular rectangle, **9**, where two cofacial binding sites exist. Similarly, a triangular linker should generate a molecular triangle, and so on. Aside from exploiting **8**, and the derived supramolecular structures for molecular recognition of planar d^8 complexes and aromatic molecules, these systems may provide more detailed insights into the spectroscopic

(7) (a) Garcia, A. M.; Romero-Salguero, F. J.; Bassani, D. M.; Lehn, J.-M.; Baum, G.; Fenske, D. *Chem. Eur. J.* **1999**, *5*, 1803−1808. (b) Rojo, J.; Lehn, J. −M.; Baum, G.; Fenske, D.; Waldmann, O.; Müller, P. *Eur. J. Inorg. Chem.* **1999**, 517−522.

(8) (a) Saalfrank, R. W.; Hörner, B.; Stalke, D.; Salbeck, J. *Angew. Chem., Int. Ed. Engl.* **1993**, *32*, 1179−1182. (b) Saalfrank, R. W.; Burak, R.; Breit, A.; Stalke, D.; Herbst-Irmer, R.; Daub, J.; Porsch, M.; Bill, E.; Müther, M.; Trautwein, A. X. *Angew. Chem., Int. Ed. Engl.* **1994**, *33*, 1621−1623. (c) Saalfrank, R. W.; Löw, N.; Trummer, S.; Sheldrick, G. M.; Teichert, M.; Stalke, D. *Eur. J. Inorg. Chem.* **1998**, 559−563.

(9) Caulder, D. L.; Raymond, K. N. *J. Chem. Soc., Dalton Trans.* **1999**, 1185−1200.

(10) (a) Cotton, F. A.; Daniels, L. M.; Lin, C.; Murillo, C. A. *Chem. Comm.* **1999**, 841−842. (b) Cotton, F. A.; Daniels, L. M.; Lin, C.; Murillo, C. A *J. Am. Chem. Soc.* **1999**, *121*, 4538−4539. (c) Cotton, F. A.; Daniels, L. M.; Lin, C. *Inorg. Chem.* **2001**, *40*, 472−477. (d) Cotton, F. A.; Daniels, L. M.; Lin, C. *Inorg. Chem.* **2001**, *40*, 478−484. (e) Cotton, F. A.; Daniels, L. M.; Lin, C. *Inorg. Chem.* **2001**, *40*, 575−577.

(11) (a) Fujita, M. *Acc. Chem. Res.* **1999**, *32*, 53−61. (b) Fujita, M. *Chem. Soc. Rev.* **1998**, *27*, 417−425. (c) Fujita, M.; Ogura, K. *Coord. Chem. Rev.* **1996**, *148*, 249−264.

(12) (a) Stang, P. J.; Olenyuk, B. *Acc. Chem. Res.* **1997**, *30*, 502−518. (b) Stang, P. J. *Chem. Eur. J.* **1998**, *4*, 19−27.

(13) Fujita, M.; Yazaki, J.; Ogura, K. *J. Am. Chem. Soc.* **1990**, *112*, 5645−5647.

(14) (a) Fujita, M.; Fujita, N.; Ogura, K.; Yamaguchi, K. *Nature* **1999**, *400*, 52−55. (b) Fujita, M.; Nagao, S.; Ogura, K. *J. Am. Chem. Soc.* **1995**, *117*, 1649−1650.

(15) (a) Klaussmeyer, K. K.; Wilson, S. R.; Rauchfuss, T. B. *J. Am. Chem. Soc.* **1999**, *121*, 2705−2711. (b) Klaussmeyer, K. K.; Rauchfuss, T. B.; Wilson, S. R. *Angew. Chem., Int. Ed.* **1998**, *37*, 1694−1696. (c) Roche, S.; Hasalm, C.; Adams, H.; Heath, S. L.; Thomas, J. A. *J. Chem. Soc., Chem. Commun.* **1998**, 1681−1682.

(16) (a) Connick, W. B.; Henling, L. M.; Marsh, R. E.; Gray, H. B. *Inorg. Chem.* **1996**, *35*, 6261−6265. (b) Connick, W. B.; Marsh, R. E.; Schaefer, W. P.; Gray, H. B. *Inorg. Chem.* **1997**, *36*, 913−922. (c) Houlding, V. H.; Miskowski, V. M. *Coord. Chem. Rev.* **1991**, *111*, 145−152. (d) Rice, S. F.; Miskowski, V. M.; Gray, H. B. *Inorg. Chem.* **1988**, *27*, 4704−4708. (e) Miller, J. R. *J. Chem. Soc.* **1961**, 4452−4457. (f) Bailey, J. A.; Miskowski, V. M.; Gray, H. B. *Inorg. Chem.* **1993**, *32*, 369−370. (g) Hegmans, A.; Zangrando, E.; Freisinger, E.; Pichierri, F.; Randaccio, L.; Mealli, C.; Gerdan, M.; Trautwien, A. X.; Lippert, B. *Chem. Eur. J.* **1999**, *5*, 3010−3018.

provenance of electronic transitions of stacked d^8 complexes.[16] Because complexes of the types, **8**, **9**, and others, may carry charge, the cofacial disposition of the metals should allow for the incorporation of negatively charged ligands and complexes, X^{m-}, into the molecular clefts as illustrated in, **10**, for the spacer-chelator, **8**.

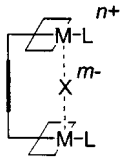

10

We report here the synthesis of a spacer-terpyridyl chelator, the formation of molecular rectangles, and the stabilities of various guests in the cofacial molecular cleft.

Design. On the basis of previous work, three spacers were considered, the naphthalene moiety, **11**, and the system, **12**, together with its oxidized analogue, **13**. The spacer, **11**,

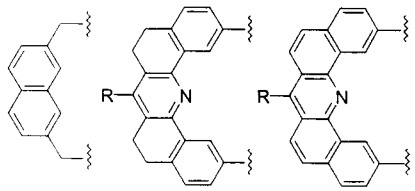

11 **12** **13**

incorporating two acetylacetonate chelators, was found by Maverick to give the di-Cu^{2+} cofacial complex, **14**, which was capable of coordinating, for example, DABCO (diazobicyclo-[2.2.2]octane) as shown.[17] By appending large aromatic groups at the positions shown in the spacers, **12** and **13**, the resultant so-called "molecular tweezers" were shown to incorporate aromatic molecules between the two cofacial aromatic groups.[18]

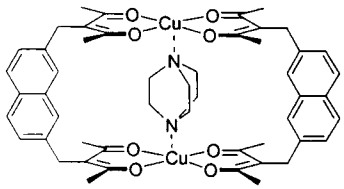

14

Because spacers of the type, **11**, are more readily prepared than **12** and **13**, the spacer-chelator, **15**, was prepared initially. Whereas Pd^{2+} and Pt^{2+} complexes could be easily prepared, it was found that the complexes failed to give a molecular rectangle using, for example, the 4,4′-dipyridyl linker. Other experiments were performed which led to the conclusion that spacer-chelators of the type, **11**, were too flexible to provide the desired supramolecular assemblies or to act as a receptor for incarcerating molecules. It thus appeared that more rigid spacers, such as **12** or **13**, were required.

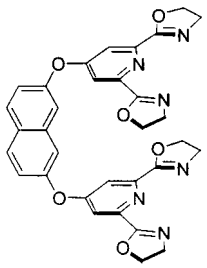

15

For a variety of reasons, including its planar geometry and its extensively known coordination chemistry, the tridentate chelator, 2,2′:6,2″-terpyridine, joined to the spacer at its 7-position was selected. The solubilities of the bis-terpyridyl spacer-chelators, however, were dependent on the nature of R in **12** and **13**. The bis-terpyridyl spacer-chelator bearing a 4-*tert*-butylphenyl R-group of the reduced spacer, **12**, was prepared, but it proved to be poorly soluble in all common solvents, and consequently, it was difficult to purify and to carry out further reactions. This paper reports the preparation of the two spacer-chelators, **16** and **17**. With the presence of the 3,5-di-*tert*-butylphenyl group, the spacer-chelator, **16**, was found to be conveniently soluble, about 200 times more soluble in CH_2Cl_2 than the 4-*tert*-butylphenyl analogue.

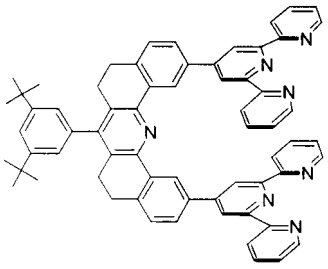

16

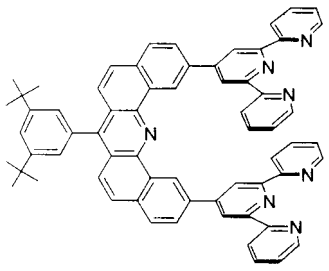

17

Results and Discussion

Spacer-Chelator Synthesis. The synthesis of **16** and **17** followed many of the procedures described previously for analogous compounds. The synthetic steps are outlined in Scheme 1. Reaction of bromobenzene with succinic anhydride under Friedel−Crafts conditions[19] gave the acylated product, **18**, which, in turn, was converted to **19** using a modified Wolff−Kishner procedure.[20] Cyclization of **19** with polyphosphoric acid[19a] gave the ketone, **20**, which was protected as a cyclic ketal,[23] **21**. The terpyridyl triflate (terpyOTf) was prepared by modifications of reported procedures.[21,22] Coupling of **21** with terpyridyl precursors required special conditions. Lithiation of **21** with *t*-BuLi[18a] proceeded well, but attempts to couple this

(17) (a) del Roario Benites, M.; Fronczek, F. R.; Hammer, R. P.; Maverick, A. W. *Inorg. Chem.* **1997**, *36*, 5826−5831. (b) Maverick, A. W.; Ivie, M. L.; Waggenspack, J. H.; Fronczek, F. R. *Inorg. Chem.* **1990**, *29*, 2403−2409.

(18) (a) Zimmerman, S. C.; VanZyl, C. M.; Hamilton, G. S. *J. Am. Chem. Soc.* **1989**, *111*, 1373−1381. (b) Zimmerman, S. C.; Zeng, Z.; Wu, W.; Reichert, D. E. *J. Am. Chem. Soc.* **1991**, *113*, 183−196. (c) Zimmerman, S. C. *Tetrahedron Lett.* **1988**, *29*, 983−986. (d) Klärner, F.-G.; Burkert, U.; Kamieth, M.; Boese, R.; Benet-Bucholz, J. *Chem. Eur. J.* **1999**, *5*, 1700−1705.

(19) (a) Newman, M. S.; Seshadri, S. *J. Org. Chem.* **1962**, *27*, 76−78. (b) Fieser, L. F.; Seligman, A. M. *J. Am. Chem. Soc.* **1938**, *60*, 170−177.

(20) Minlon, H. *J. Am. Chem. Soc.* **1946**, *68*, 2487−2488.

Scheme 1[a]

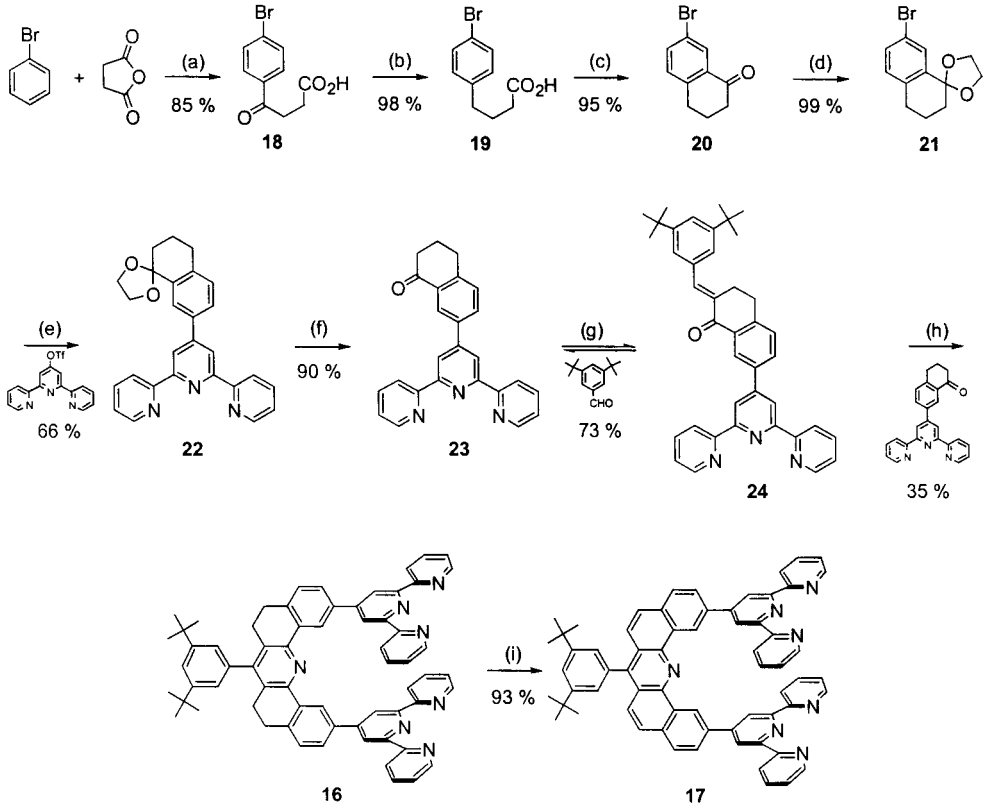

[a] (a) $AlCl_3$/*o*-dichlorobenzene, 95 °C, 7 h; HCl/H_2O. (b) KOH, NH_2NH_2/triethyleneglycol, 200 °C, 2 h; HCl. (c) Polyphosphoric acid, 90 °C, 2 h. (d) Ethyleneglycol, *p*-TsOH/benzene, 105 °C, 48 h. (e) *t*-BuLi/THF, −78 °C, $ZnCl_2$; terpy-OTf, [$Pd(PPh_3)_4$], 80 °C, 48 h; KCN/DMSO−H_2O, 120 °C, 1 h. (f) *p*-TsOH/acetone−H_2O, 25 °C, 72 h. (g) 4% KOH/MeOH−THF, 36 h. (h) BF_3·Et_2O, 115 °C, 8 h; NH_3/MeOH−CH_2Cl_2, 25 °C, 48 h. (i) DDQ/1,4-dioxane, 120 °C, 24 h.

lithium species with either terpyOTf or its ketone precursor[21,22] led to the formation of intractable, highly colored products. Replacing the lithium for MgBr gave similar intractable products. It was found that the ZnCl species of **21** did not react with terpyOTf, but the coupling was catalyzed by [$Pd(PPh_3)_4$]. This coupling has advantages and disadvantages. Addition of $ZnCl_2$ to the lithium salt of **21** causes a color change from yellow to colorless, but addition of terpyOTf to this solution in THF leads to the almost complete precipitation of, presumably, a terpyOTf−zinc complex which, as a result, retards the rate of coupling. The advantage of the procedure is that, upon completion of the coupling, the product can be purified by simple filtration of the insoluble zinc complex of the coupled product. The zinc complex is decomposed with cyanide ions to give **22** as a powder. The protecting group is readily removed to give the ketone, **23**, as a crystalline solid. Formation of **24** was found to be under thermodynamic control for the conditions used, and attempts at conventional workups led to the isolation of the starting materials and a low yield of product; the amount depended on the time and nature of the workup. To obtain a good yield of **24**, it was necessary to allow the aldehyde[23] and the ketone **23** to react in a solvent mixture in which the two starting materials are soluble but in which the product is poorly soluble. In this way, the homogeneous equilibrium was displaced to the heterogeneously deposited product.

The yield of the penultimate product, **16**, was modest. Reaction of the tetralone, **23**, with **24** in boron trifluoride etherate[24] gives the pyrylium BF_4^- salt which can be isolated as a yellow-orange solid. This material was allowed to react with methanolic ammonia to give **16** in a 35% overall yield based on the tetralone, **23**. The product, **16**, is in an oxidation state higher than would be expected from the coupling of **23** and **24**, and it is possible that **24** oxidizes the initially coupled product to the pyrylium salt. Consequently, an excess of **24** is used to achieve the 35% yield. Use of concentrated perchloric acid[24] for the coupling gave a lower yield. Addition of hydride abstracting agents such as trityl ions or DDQ (2,3-dichloro-5,6-dicyano-1,4-benzoquinone) to the boron trifluoride etherate reaction did not lead to a higher yield presumably because **24** is a faster oxidizing agent. The spacer-chelator, **16**, is efficiently oxidized to the all-aromatic compound, **17**, with DDQ in dioxane.

Although multiple steps are involved in the synthesis of **16** and **17**, the protected ketone, **21**, can be produced in 100 g quantities in a single sequence. Most of the subsequent steps proceed in high yield except for the coupling of **23** with **24**. Even so, gram quantities of the spacer-chelators, **16** and **17**, can be conveniently obtained.

Synthesis of Complexes. Although a number of complexes have been prepared using **16** and **17**, only certain Pd^{2+} complexes are described here because they illustrate the essential characteristics of these spacer-chelators. To prepare these Pd^{2+}

(21) Constable, E. C.; Ward, M. D. *J. Chem. Soc., Dalton Trans.* **1990**, 1405−1409.

(22) Potts, K. C.; Konwar, D. *J. Org. Chem.* **1991**, *56*, 4815−4816.

(23) Newman, M. S.; Lee, L. F. *J. Org. Chem.* **1972**, *37*, 4468−4469. We wish to express our thanks to Ron Warrener for alerting us to this procedure.

(24) (a)VanAllan, J. A.; Reynolds, G. A. *J. Org. Chem.* **1968**, *33*, 1102−1105. (b) Katritzky, A. R.; Thind, S. S. *J. Chem. Soc., Perkin Trans. 1* **1980**, 1895−1900. (c) Siemiatycki, M.; Fugnitto, R. *Bull. Chem. Soc. Fr.* **1961**, *27*, 538−540. (d) Katritzky, A. R.; Bravo-Borja, S.; El-Mowafy, A. M.; Lopez-Rodriguez, M. L. *J. Chem. Soc., Perkin Trans. 1* **1984**, 1671−1673.

Scheme 2[a]

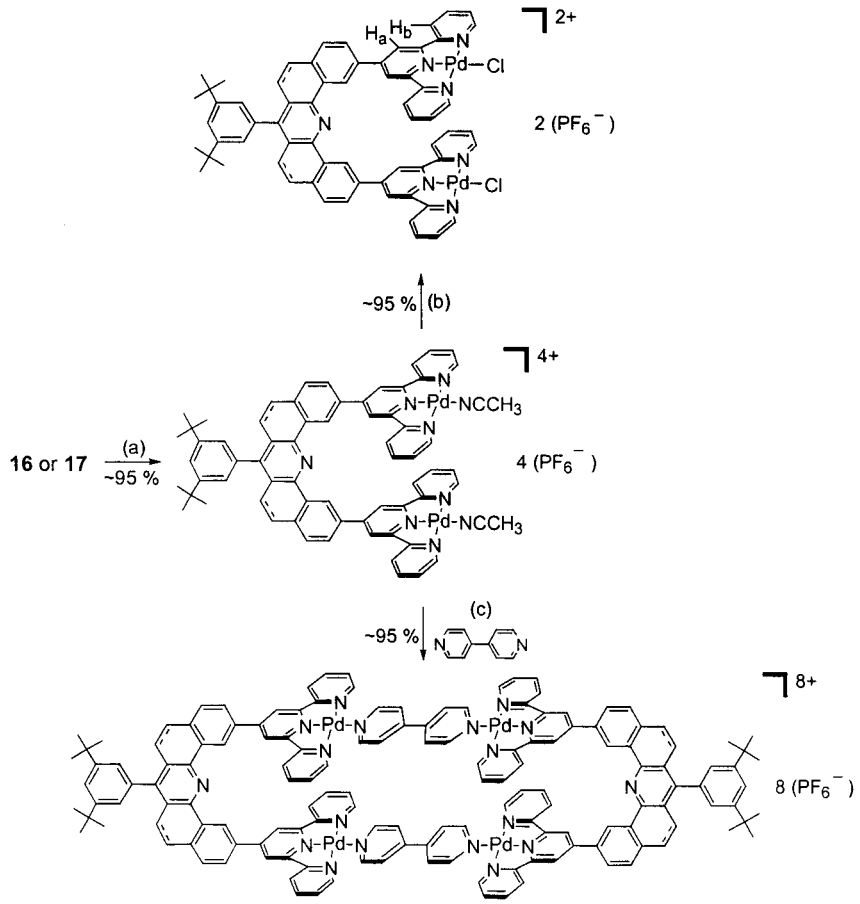

[a] (a) 2[Pd(CH$_3$CN)$_4$](PF$_6$)$_2$/CH$_3$CN, 25 °C, 4 h. (b) Et$_4$NCl/CH$_3$CN−MeOH, 25 °C, 1 h. (c) CH$_3$CN, 25 °C, 1 h.

complexes and to generate rapidly supramolecular structures, the Pd^{2+} starting material requires the coordination of labile ligands. The [Pd(CH$_3$CN)$_4$](PF$_6$)$_2$ complex was chosen as the metallating complex. It was prepared by the method outlined in eq 1, where the NO^+ ion acts as a 1-electron oxidizing agent releasing NO.[25]

$$\underset{\text{Sponge}}{\text{Pd}} \xrightarrow[\text{CH}_3\text{CN, 60 °C, 4 h}]{\text{2.1 equiv NOPF}_6} \underset{\textbf{90\%}}{[\text{Pd(CH}_3\text{CN)}_4](\text{PF}_6)_2} + \underset{}{2\ \text{NO}} \qquad (1)$$

The preparation of Pd^{2+} complexes of the spacer-chelators, **16** and **17**, is outlined in Scheme 2. In all cases, the isolated yields are essentially quantitative.

The compounds shown in Scheme 2 were also prepared as their triflate salts, from [Pd(CH$_3$CN)$_4$](OTf)$_2$,[26] but these salts were less soluble in CH$_3$CN solutions, which were used for host−guest stability measurements. The PF_6^- salt of the palladium−chloro complex of the oxidized ligand, **17**, however, was very insoluble in common solvents. It is only slightly soluble in dimethyl sulfoxide. The ^{1}H NMR spectra of the complexes are reported in the Experimental Section and conform to the structures shown. Some of the ^{1}H NMR signals are broad for the acetonitrile and chloro complexes of the reduced spacer at 20 °C in CD$_3$CN solutions, but those for the chloro complex become sharp at ∼50 °C. In the case of [(**16**)Pd$_2$(CH$_3$CN)$_2$](PF$_6$)$_4$, however, many of the ^{1}H NMR signals remain broad at 50 °C in CD$_3$CN solutions. Since this broadness is not observed for the acetonitrile complex of the oxidized spacer, the broadness in some of the peaks at 20 °C for the reduced spacer complexes may be connected with slow conformational interconversions of the reduced spacer. We discuss these conformations later. The molar conductivities of the reduced and oxidized spacer acetonitrile complexes are 334 and 384 Ω^{-1} cm^2 mole^{-1}, respectively, in acetonitrile solutions. These conductivities are in the range for 3:1 electrolytes[27] and may suggest some ion association. We have no evidence that one of the PF_6^- ions is incarcerated in the cleft, however. The chloro complex of the reduced spacer has conductivity consistent with that of a 2:1 electrolyte, namely, 235 Ω^{-1} cm^2 mole^{-1} in the same solvent.

Crystallization of these complexes proved difficult because of their tendency to form what appeared to be gels. Slow diffusion of ether into acetonitrile solutions gave microcrystalline materials for all of the complexes except for the molecular rectangle of the reduced spacer which always gave a gel. It was isolated as a powder from neat acetonitrile. Both acetonitrile complexes exhibit unusual behavior when ethyl ether, acetone, or tetrahydrofuran are added rapidly to acetonitrile solutions of the complexes. Deep orange or deep red precipitates are formed which, upon filtration, effluoresce and revert to a yellow color. Even if the yellow crystals of the oxidized spacer acetonitrile complex are exposed to ether, they turn to a deep red color and become yellow when the ether is removed. Presumably, these color changes reflect packing of the molecules in the crystal, but as yet, we have not been able to grow suitable crystals for X-ray analysis.

(25) (a)Wayland, B. B.; Schramm, R. F. *Inorg. Chem.* **1969**, *8*, 971−976. (b) Thomas, R. R.; Sen, A. In *Inorganic Syntheses*; Angelici, R. J., Ed.; John Wiley & Sons: New York, 1990; Vol. 28, pp 63−67

(26) Drent, E.; van Brockhoven, J. A. M.; Doyle, M. J. *J. Organomet. Chem.* **1991**, *417*, 235−251.

(27) Geary, W. J. *Coord. Chem. Rev.* **1971**, *7*, 81−122.

It is significant that the formation of the two molecular rectangles appears to be complete shortly after mixing of the spacer-chelator and the linker as judged by ^{1}H NMR spectroscopy. The formation of the molecular rectangles is quantitative. This behavior contrasts with the formation of the Pd^{2+} molecular squares of Fujita and Stang which form quantitatively but take hours or days to do so. Presumably, the difference is associated with having fewer elements to combine together with a predisposed structure in the case of the present rectangles. The rapid and clean formation of the present molecular rectangles suggests that more complex molecular architectures will form readily with the present systems.

That molecular rectangles are formed, rather than oligomers or polymers, is supported by their ^{1}H NMR spectra which, on an NMR time scale, are consistent with molecules of D_{2h} symmetry and by their ESI-MS spectra which provide a series of ion signals consistent with their molecular weights.

Molecular Recognition. The dichloro di-PF_6 reduced receptor, [(**16**)Pd_2Cl_2]$(PF_6)_2$ (Scheme 2), was employed to investigate its ability to incarcerate substrates into the cleft. Acetonitrile was used as the solvent, and a variety of planar guests was examined including, **25**, **26**,[28] **27**, and **28**. The substrates **25**, **26**, and **27** are a series of planar metal complexes which served to examine the effect of the overall charge on molecular recognition by the dipositively charged receptor. It is recognized, however, that additional factors could influence the stability of the host−guest complex in this series. Substrate, **28**, was investigated to ascertain the effect of π-stacking dispersion forces in the absence of potential metal−metal interactions which may exist, in addition to π-stacking, in the metal complexes.

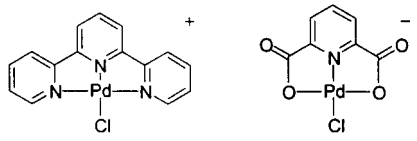

25

26

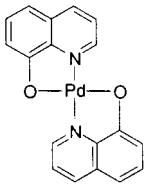

27

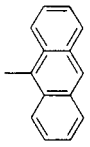

28

Addition of **25** to the dichloro receptor, [(**16**)Pd_2Cl_2]$(PF_6)_2$, at 20 °C did not reveal any association. There were no significant shifts in the ^{1}H NMR signals of either the potential guest or host and the visible absorption spectra obeyed Beer's law. Complexes of the type, **25**, tend to stack in their crystalline forms,[29] and it is possible that the absence of observable interaction in this case is due to electrostatic repulsion between the positively charged host and guest. The opposite should be the case for the interaction of the negatively charged potential guest, **26**, and the positively charged host. Addition of **26** to the host, however, led to immediate precipitation of a gelatinous product in CH_3CN solutions. This product remains insoluble even in hot dimethylformamide. Although it is clear that a salt of the host and guest is formed, the question of whether the guest resides in the cleft of the host could not be established because of insolubility.

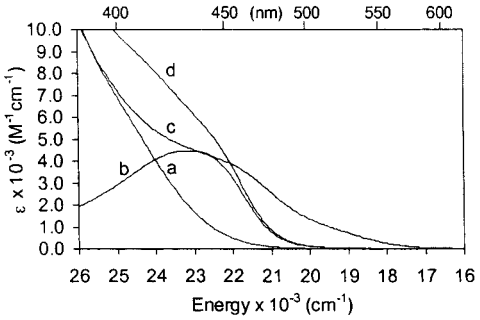

Figure 1. Absorption spectra for (a) [(**16**)Pd_2Cl_2]$(PF_6)_2$, (2.74 mM), (b) **27**, (2.74 mM), (c) 1:1 solution of [(**16**)Pd_2Cl_2]$(PF_6)_2$, and **27**, (2.74 mM each), and (d) normalized sum of a and b.

The neutral compound, **27**, does form an adduct with [(**16**)Pd_2Cl_2]$(PF_6)_2$, but the study was circumscribed by the low solubility of **27**. Consistent with host−guest formation is the observation that **27** becomes more soluble in CH_3CN solutions when [(**16**)Pd_2Cl_2]$(PF_6)_2$ is present, up to the point when 1 equiv of **27** is added to a host solution. Using 2.74×10^{-3} M solutions of the [(**16**)Pd_2Cl_2]$(PF_6)_2$ receptor and sequential additions of **27** causes substantial chemical shifts of certain protons of the host and those of the guest. These studies were performed at 57 °C because, at ambient temperatures, the ^{1}H NMR signals (at 500 MHz) which showed the greatest shifts upon host−guest association were very broad. The line broadness may indicate that guest exchanges with the host at a rate comparable to the ^{1}H NMR time scale, but it is also possible that conformational interconversions of the host−guest complex could lead to this line-broadening. At 57 °C all ^{1}H NMR signals are sufficiently sharp to determine the chemical shifts. The maximum chemical shifts for the H_a and H_b protons (Scheme 2) of the host were 0.49 and 0.39 ppm, respectively, and one of the protons of the guest has a maximum shift of 0.66 ppm. A plot of chemical shift versus host−guest molar ratio[30] gave a straight line until a ratio of 1:1 was achieved. After this ratio, very small changes in chemical shift were observed but beyond a 1:1 host−guest ratio not all of the guest was in solution. Consequently, it was not possible to determine an equilibrium constant, but it is clear that a strong 1:1 complex is formed. The visible absorption spectra confirm a host−guest association. Figure 1 shows four spectra, one of the host alone, one of the guest alone, a normalized sum of these two spectra and the spectrum observed for a 1:1 ratio of host and guest. It is clear that the association complex gives a spectrum that is not the sum of its parts. The host−guest spectrum is weaker in intensity above about 23 000 cm^{-1} but has significant absorption below 20 000 cm^{-1} where neither the isolated host nor guest absorb. These observations indicate that the electronic states of the host or the guest have been modified by association and a new or modified existing electronic transition below 20 000 cm^{-1} is generated by association.

Association of **28** with [(**16**)Pd_2Cl_2]$(PF_6)_2$ follows a pattern similar to that observed in the association of **27** but, in this case, **28** is sufficiently soluble for a complete study of host−guest stability. The "mole ratio method"[30] was used to determine host−guest association at 23 °C. The concentration of the receptor (5×10^{-3} M) was kept constant, while the concentra-

(28) Espinet, P.; Miguel, J. A.; Garciá-Grande, S.; Miguel, D. *Inorg. Chem.* **1996**, *35*, 2287−2291.

(29) (a) Bailey, J. A.; Hill, M. G.; Marsh, R. E.; Miskowski, V. M.; Schaefer, W. P.; Gray, H. B. *Inorg. Chem.* **1995**, *34*, 4591−4599. (b) Cosar, S.; Janik, M. B. L.; Flock, M.; Freisinger, E.; Farkas, E.; Lippert, B. *J. Chem. Soc., Dalton Trans.* **1999**, 2329−2336. (c) Yip, H.-K.; Cheng, K.-K.; Che, C.-M. *J. Chem. Soc., Dalton Trans.* **1993**, 2933−2938.

(30) Meyer, A. S.; Ayres, G. H. *J. Am. Chem. Soc.* **1957**, *79*, 49−53.

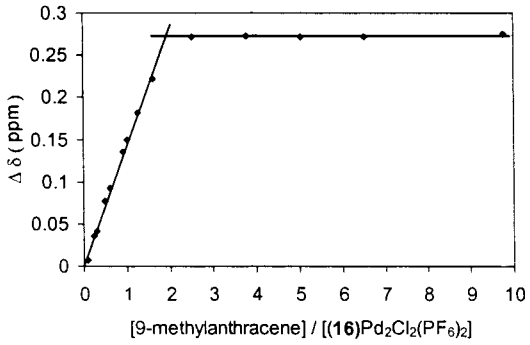

Figure 2. ^{1}H NMR stoichiometry determination of the adducts formed by [(**16**)Pd_2Cl_2]$(PF_6)_2$ with **28**. The experiments were performed in CD_3-CN at 23 °C with concentration of [(**16**)Pd_2Cl_2]$(PF_6)_2$ constant at 5.00 mM and the concentration of **28** varied between 0.5 mM and 50 mM.

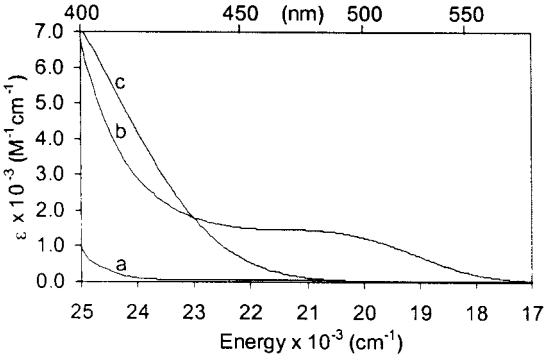

Figure 3. Absorption spectra for (a) **28**, (50.0 mM), (b) **28**, (50.0 mM) and [(**16**)Pd_2Cl_2]$(PF_6)_2$, (5.00 mM), and (c) [(**16**)Pd_2Cl_2]$(PF_6)_2$, (5.00 mM).

tion of **28** was varied from 5×10^{-4} to 5×10^{-2} M. Changes in chemical shifts for a number of the guest and host protons were observed. Plots of changes in chemical shifts ($\Delta\delta$) for each of the shifted protons versus molar ratio were made. All of these plots indicated 2:1 guest-to-host association. A plot of the change in chemical shift versus mole ratio for the H_a protons is shown in Figure 2 where the slope-break occurs at the 2:1 ratio. From these data, the two equilibrium constants for association were estimated[31] to be 650 ± 50 M^{-1} for the first association and 200 ± 50 M^{-1} for the second. The firm conclusion, however, is that strong association occurs for both the 1:1 and 2:1 complexes.

The visible absorption spectra are shown in Figure 3 for **28**, the receptor and for the receptor−guest complexes at the maximum concentration of guest (5×10^{-2} M of guest and 5×10^{-3} M of receptor). This last spectrum varies with receptor-to-guest ratio, but isobestic points are not observed. It is clear that the association spectrum of the receptor−guest complexes is distinct; above 23 000 cm^{-1} the complexes show absorption intensity weaker than the receptor, and below about 21 000 cm^{-1} a new or modified existing absorption band is observed. This spectrum reflects the yellow-to-red color change observed when **28** is added to the receptor. Addition of **28** to the free ligand, **16**, does not lead to a color change, nor are there any shifts in the proton resonances which would indicate association. The free ligand, **16**, compared to the complex [(**16**)Pd_2Cl_2]$^{2+}$, has more degrees of freedom, and this, to some extent, may account for the lack of association, but additional factors are likely to lead to the stability of the incarcerated guests in [(**16**)Pd_2Cl_2]$^{2+}$.

It is generally assumed[32] that the binding in aromatic excimers (π-stacked molecules) is largely due to exciton resonance configurational mixing with the ground state. Contributions from the Coulombic interactions of the excited state molecular ions are regarded as a lesser contribution to the excimer stability. Exciton configurational mixing is likely to play an important role in the stabilities of host−guest complexes formed by [(**16**)Pd_2Cl_2]$^{2+}$ and **27** and **28**, but additional contributions may play a role. In the case of the palladium complex, **27**, there exists the possibility of stabilizing metal−metal bond formation between the metals of the host and the guest.[33] Further, the presence of positive charge in the receptor may stabilize guest association, for both **27** and **28**, by dipole induction. Interactions of the kind discussed are clearly the source of the additional electronic absorptions observed for the host−guest complexes (Figures 1 and 3), but it is not clear whether these bands arise from modifications to existing bands or are due to new transitions peculiar to the host−guest complex.

Crystal Structure. Attempts to obtain crystals suitable for X-ray diffraction of the free ligands, **16** and **17**, and of their acetonitrile or chloro palladium complexes were not successful. Although well-formed needles were obtained for many of these compounds, the materials were very weakly diffracting and proved unsuitable for X-ray diffraction. The same was the case for the molecular rectangles. As noted, the neutral complex, **27**, does form a 1:1 adduct with [(**16**)Pd_2Cl_2]$(PF_6)_2$ in CH_3CN solutions, but attempts to crystallize the adduct by diffusion of methanol led to the crystallization of the host and guest, separately. It is clear that, for host−guest adducts to crystallize, a solvent mixture is required where the solubility product of the host−guest adduct is less than those of the constituent parts. This favorable circumstance was found when a CH_3CN solution of 1 equiv of [(**16**)Pd_2Cl_2]$(PF_6)_2$ and 2 equiv of 9-methylanthracene (9-MA) was vapor diffused with methanol. Orange crystals, having the formula [(**16**)Pd_2Cl_2]$(PF_6)_2$·$(9\text{-MA})_2$·$(CH_3CN)_{1.5}$, formed. These crystals effloresce, are fragile, and scatter X-rays weakly, but they did provide a satisfactory crystal structure of the host−guest complex. Crystallographic data are listed in Table 1 and selected bond lengths and angles are provided in Table 2. Hydrogen atoms were not located. The bond lengths and angles correspond to those usually found for terpyridyl palladium complexes[34] and for the organic parts of the molecule.

Figure 4 illustrates three perspectives of the molecular adduct where the CH_3CN molecules and the PF_6^- ions are removed. The reduced rings of the receptor exist in a chiral, as opposed to meso, conformation. This chirality is transmitted to the essentially coparallel terpy−Pd−Cl units which, as a consequence, are aligned in a splayed (chiral) configuration (Figure 4). As we describe presently, however, the crystal is racemic with both chiralities present in the unit cell as required for the space group. The molecular structure of the receptor is twisted. The dihedral angles between the spacer and the terpy−Pd(1)−Cl and terpy−Pd(2)−Cl units are −39.0° and −36.5°, respectively. The dihedral angle between the spacer and the 3,5-di-*tert*-butyl-phenyl group is −53.4°, possibly because of interaction with neighboring 9-MA molecule. The distance between the two carbon atoms of the spacer to which the two terpy−Pd−Cl units are joined is 7.07 Å, as expected. Because of the twist

(31) Kneeland, D. M.; Ariga, K.; Lynch, V. M.; Huang, C.-Y.; Anslyn, E. V. *J. Am. Chem. Soc.* **1993**, *115*, 10042−10055.

(32) (a) Murrell, J. N.; Tanaka, J. *Mol. Phys.* **1964**, *45*, 363. (b) Lim, E. C. *Acc. Chem. Res.* **1987**, *20*, 8−17.

(33) (a)Krogmann, K. *Angew. Chem., Int. Ed. Engl.* **1969**, *8*, 35−42. (b) Gliemann, G.; Yersin, H. *Struct. Bonding* **1985**, *62*, 87−153. (c) Miller, J. S. *Extended Linear Chain Compounds;* Plenum Press: New York, 1982−1983; Vols. 1−3.

(34) Intille, G. M., Pfluger, C. E., Baker, W. A. Jr., *J. Cryst. Mol. Struct.* **1973**, *3*, 47−54.

Table 1. Crystallographic Data for $[(\mathbf{16})Pd_2Cl_2](PF_6)_2\cdot(9\text{-MA})_2\cdot(CH_3CN)_{1.5}$

compound	$[(\mathbf{16})Pd_2Cl_2](PF_6)_2\cdot(9\text{-MA})_2\cdot(CH_3CN)_{1.5}$
formula	$C_{95}H_{83.5}Cl_2F_{12}N_{8.5}P_2Pd_2$
formula weight	1917.84
space group	$P\bar{1}$
a, Å	12.1466(4)
b, Å	14.3345(5)
c, Å	27.9157(9)
α, deg	79.434(2)
β, deg	77.962(3)
γ, deg	82.151(2)
V, Å^3	4648.6(3)
Z, *Z*′	2
cryst. color, habit	orange block
D(calc), g cm^{-3}	1.370
μ(Mo Kα), cm^{-1}	5.52
temp, K	173(2)
diffractometer	Siemens P4/CCD
radiation	Mo Kα ($\lambda = 0.71073$ Å)
$R(F)$, %[a]	9.29
$R(wF^2)$, %[a]	21.57

[a] Quantity minimized $= R(wF^2) = \sum[w(F_o^2 - F_c^2)^2]/\sum[(wF_o^2)^2]^{1/2}$; $R = \sum\Delta/\sum(F_o)$, $\Delta = |(F_o - F_c)|$. $w = 1/[\sigma^2(F_o^2) + (aP)^2 + bP]$, $P = [2F_c^2 + \max(F_o,0)]/3$.

Table 2. Selected Bond Lengths and Angles for $[(\mathbf{16})Pd_2Cl_2](PF_6)_2\cdot(9\text{-MA})_2\cdot(CH_3CN)_{1.5}$

	Bond Lengths (Å)		
N(2)−Pd(1)	1.916(8)	N(5)−Pd(2)	1.899(7)
N(3)−Pd(1)	2.044(8)	N(6)−Pd(2)	2.002(8)
N(4)−Pd(1)	2.005(9)	N(7)−Pd(2)	2.042(8)
Cl(1)−Pd(1)	2.294(3)	Cl(2)−Pd(2)	2.288(2)
	Bond Angles (deg)		
N(2)−Pd(1)-N(4)	81.4(3)	N(5)−Pd(2)-N(6)	80.4(3)
N(2)−Pd(1)-N(3)	80.7(3)	N(5)−Pd(2)-N(7)	82.1(3)
N(4)−Pd(1)-N(3)	162.1(3)	N(6)−Pd(2)-N(7)	162.2(3)
N(2)−Pd(1)-Cl(1)	179.0(3)	N(5)−Pd(2)-Cl(2)	177.5(2)
N(4)−Pd(1)-Cl(1)	99.2(2)	N(6)−Pd(2)-Cl(2)	99.6(2)
N(3)−Pd(1)-Cl(1)	98.7(2)	N(7)−Pd(2)-Cl(2)	98.0(2)

between the spacer and the chelators, the interplanar separation of the two terpy−Pd−Cl units will decrease as the spacer-chelator dihedral angles deviate from 90°. Thus, the interplanar separation of the two terpy−Pd−Cl units is adjustable, but as the separation decreases, the two terpy−Pd−Cl molecular planes will slide away from each other, diminishing the cleft volume.

One of the 9-MA molecules lies almost fully within the molecular cleft, whereas the other lies outside the cleft. The probable reasons for the position of the 9-MA outside of the cleft will become apparent presently. The incarcerated 9-MA is nearly coplanar with the two coparallel terpy−Pd−Cl units which enclose it. Further, this 9-MA is nearly equidistant from the two terpy−Pd−Cl units, being 3.44 Å from terpy−Pd(1)−Cl and 3.48 Å from terpy−Pd(2)−Cl. Thus, the interplanar separations are those expected for ideal *π*-stacking, a circumstance which may, in part, account for the observed high first stability constant. Whereas the two terpy−Pd−Cl units are not eclipsed because of the twist of the spacer, the Pd−Pd separation is 6.92 Å which is equal to the sum of the interplanar host−guest separations (3.44 and 3.48 Å).

The overall crystal structure has additional interesting features. Going beyond the unit cell, the structure reveals a variety of molecular-stacking interactions. Figure 5 illustrates the extended structure and the outline of the unit cell. As before, the CH_3CN molecules and the PF_6^- ions are omitted, and the hydrogen atoms are excluded. Figure 5 shows that two terpy−Pd−Cl units from different receptor molecules, namely those carrying Pd(1) and Pd(1A), are cofacially disposed. The mean distance between the planes is 3.55 Å. These two terpy−Pd−Cl units are displaced with the chloro ligands lying above the central pyridine of the terpy ligand of the neighboring, cofacial terpy−Pd−Cl unit. Consequently, the two palladium atoms (Pd(1) and Pd(1A)), when viewed orthogonally to the terpy−Pd−Cl planes are not eclipsed but are displaced by 1.27 Å from each other in the direction of the central pyridine group of the neighboring terpy−Pd−Cl units. Although the two palladium ions, (Pd(1) and Pd(1A)), are displaced from each other, their separation is 3.71 Å which may indicate weak metal−metal interaction with the axial metal orbitals. The stacking of these two terpy−Pd−Cl units is reminiscent of the stacking observed for the crystal structures of the $[Pd(terpy)Cl]^+$ and the $[Pt(terpy)Cl]^+$ ions.[29a,34] The 9-MA molecules outside of the cleft also appear to be involved in *π*-stacking with the outer faces of the terpy−Pd−Cl units of the two hosts in the unit cell as illustrated in Figure 5. These 9-MA molecules lie approximately parallel to the respective terpy−Pd(2A)-Cl and terpy−Pd(2)−Cl units. The 9-MA molecules are separated from the terpy−Pd−Cl fragments by 3.48 Å. Thus, the overall crystal structure reveals three types of *π*-stacking: incarceration of 9-MA in the cleft, stacking of the terpy−Pd−Cl units of different molecules, and stacking of 9-MA molecules with the outside faces of the terpy−Pd−Cl units. Because these *π*-stacking interactions are in a roughly coparallel alignment with an average interplanar separation of about 3.5 Å, the crystal structure reveals a column of eight *π*-interacting units.

These observations may suggest the structure of the 2:1 adduct formed by $[(\mathbf{16})Pd_2Cl_2]^{2+}$ and 9-MA in CH_3CN solutions. As the crystal structure indicates, the volume of 9-MA is close to that provided by the cleft of $[(\mathbf{16})Pd_2Cl_2]^{2+}$, and it is not obvious what energetic advantage would accrue if the cleft were to accept two, partially incarcerated, 9-MA molecules. We are inclined to speculate that, in CH_3CN solution, one of the 9-MA molecules is fully incarcerated and that the other interacts with the outer face of a terpy−Pd−Cl unit, essentially the interactions observed in the crystal structure. Although the stacking of the molecules in the crystal structure is referred to as *π*-stacking, we do not necessarily imply that all of the attractive interactions are due to dispersion forces as is assumed for the stacking of neutral aromatic molecules. The extensive stacking observed in the crystal may suggest that induced dipoles caused by the charged host may be significant.

Experimental Section

General Procedures. All reagents were obtained from commercial suppliers and were used without further purification. All reactions were performed under an atmosphere of argon, unless otherwise specified. Electronic absorption spectra were obtained using a Perkin-Elmer Lambda 6 UV/vis spectrophotometer. Elemental analyses were performed by Desert Analytics, Inc., Tucson, Arizona. Conductance measurements were performed at 23 °C in dry acetonitrile on 1×10^{-3} molar samples using an YSI Scientific Model 35 conductance meter. ^{1}H and ^{13}C NMR spectra were recorded using a Bruker DRX400, a Bruker DRX500, or a Bruker DMX500 Fourier transform spectrometer, as indicated for each substrate. Chemical shifts, *δ*, are reported in ppm, referenced to TMS, and coupling constants, *J*, are reported in hertz. ESI-mass spectrometry was performed using a Finnigan LCQ. Melting points are uncorrected. Acetonitrile was dried over CaH_2, tetrahydrofuran was dried over potassium/benzophenone ketyl, diethyl ether was dried over sodium/benzophenone ketyl, and methylene chloride was dried over CaH_2. Thin-layer chromatography was carried out using precoated silica gel (Whatman PE SIL G/UV) or precoated aluminum oxide (J. T. Baker, aluminum oxide IB−F). Silica gel 60 Å (Merck, 230−400 mesh) and aluminum oxide 58 Å (either activated, basic, Brockman I or activated, neutral, Brockman I) were used for chromatography as indicated. Celite is J.T. Baker Celite 503.

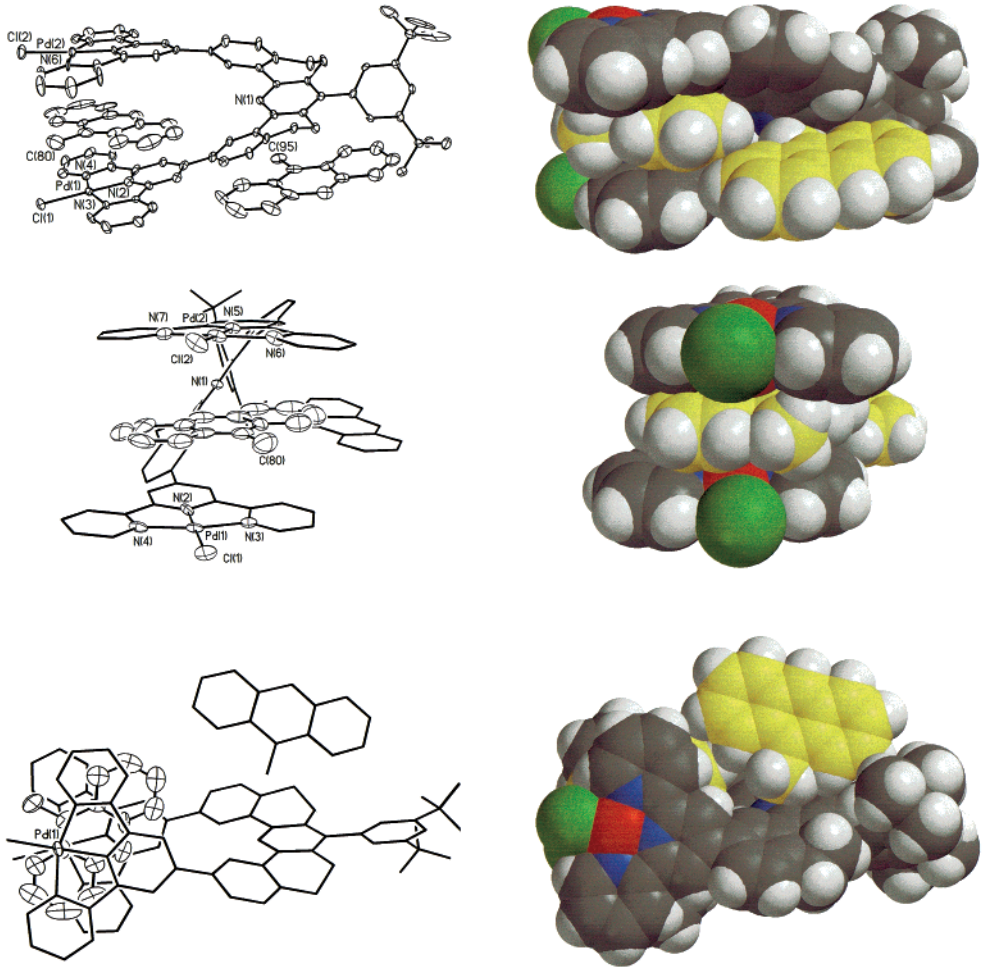

Figure 4. Three perspectives of the molecular adduct, [(**16**)Pd_2Cl_2(9-MA)]$^{2+}$·9-MA. In the left column are shown, a "side" view as 25% probability thermal ellipsoids, a "front" view and a "top" view where incarcerated 9-MA is shown as thermal ellipsoids in all cases. The right column represents these illustrations as space filling models with hydrogen atoms included. The color code is: H, white; Pd, red; Cl, green; receptor C, gray-black; 9-MA carbons are in yellow for clarity.

The following compounds were prepared by modifications of known procedures:

4-(4-bromo-phenyl)-4-oxo-butyric acid (**18**),[19] 4-(4-bromo-phenyl)-butyric acid (**19**),[19,20] 7-bromo-3,4-dihydro-2H-naphthalen-1-one (**20**),[19] 7-bromo-1,2,3,4-tetrahydronaphthalene-1-spiro-2′-(1′,3′-dioxacyclopentane) (**21**),[18a] 2,6-di-2-pyridyl-4(1*H*)-pyridone,[21,22] trifluoro-methanesulfonic acid [2,2′;6′,2″]terpyridin-4′-yl ester,[22] 3,5-di-*tert*-butylbenzaldehyde.[23]

7-[2,2′,6′,2″]Terpyridin-4′-yl-1,2,3,4 tetrahydronaphthalene-1-spiro-2′-(1′,3′-dioxacyclopentane) (22). A 200 mL flask was flame dried under a continuous stream of argon. The flask was charged with a solution of the protected tetralone, **21**, (3.00 g, 11.2 mmol) in tetrahydrofuran (80 mL). This colorless solution was cooled to −78 °C using a dry ice/acetone bath and was stirred at this temperature for 15 min. *tert*-Butyllithium (14.4 mL, 1.7 M in pentane, 24.5 mmol) was then added. The addition resulted in the formation of a bright yellow-colored solution. The reaction was stirred at −78 °C for 40 min. To this solution was added a solution of $ZnCl_2$ (23.4 mL, 0.5 M in THF, 11.7 mmol). The reaction was stirred for 40 min at −78 °C. To the now colorless solution at −78 °C, was added terpyOTf (4.68 g, 12.3 mmol) followed immediately by tetrakis(triphenylphosphine)palladium(0) (0.770 g, 0.669 mmol). Upon addition of the terpyOTf, the reaction color became red-purple. The reaction was stirred for a few min at −78 °C before being permitted to warm to 0 °C. As the reaction warmed, the color became more purple. Once the reaction reached 0 °C, a light colored precipitate began to form. The reaction was then heated to 80 °C on an oil bath and was refluxed for 48 h. During this time, the color of the solution changed to beige, and more precipitate was formed. After this period, the reaction was allowed to cool to room temperature. The beige-colored precipitate was collected by filtration and was washed with methanol (35 mL) followed by methylene chloride (50 mL) and finally with hexanes (25 mL). The beige solid was suspended in DMSO (45 mL), and the mixture was heated to 120 °C in an oil bath to give a red solution. To this solution was added KCN (7.25 g, 0.112 mol), and then water (8.5 mL) was added dropwise over 30 min. During this time the color lightened to yellow, the KCN dissolved, and the product began to precipitate. Water (36.5 mL) was then added to the reaction mixture, and the reaction was stirred for another 30 min as more precipitate formed. The reaction was permitted to cool slowly to room temperature. The product was filtered and was washed with methanol (45 mL) followed by hexanes (15 mL). The product was then dried under vacuum to yield an off-white solid of sufficient purity to use in the next step (3.10 g, 66.2%). ^{1}H NMR (CD_2Cl_2, 400 MHz): δ 2.00 (m, 4H), 2.88 (m, 2H), 4.21 (m, 4H), 7.29 (d, $J = 7.99$, 1H), 7.37 (m, 2H), 7.76 (dd, $J_1 = 2.02$, $J_2 = 5.95$, 1H), 7.97 (d, $J = 1.93$, 1H), 8.67−8.73 (m, 4H). ^{13}C NMR (CD_2Cl_2, 125 MHz): δ 21.05, 29.34, 33.80, 65.53, 107.34, 119.04, 121.52, 124.21, 125.37, 127.61, 129.71, 136.86, 137.18, 138.83, 140.28, 149.57, 150.60, 156.37, 156.64.

7-[4′-[2,2′;6′,2″]Terpyridine]-3,4-dihydro-2H-naphthalen-1-one (23). A 250 mL flask was charged with the coupled product, **22**, (6.20 g, 14.7 mmol) suspended in a mixture of acetone (150 mL) and distilled water (5 mL). To this white suspension was added *p*-toluenesulfonic acid (0.300 g, 1.47 mmol). The reaction was stirred at room temperature for 4 h and was then heated to reflux, which dissolved the remaining material. The reaction was then allowed to cool to room temperature and was stirred for another 68 h, after which time the solvent was removed to yield a white residue. This solid was dissolved in methylene

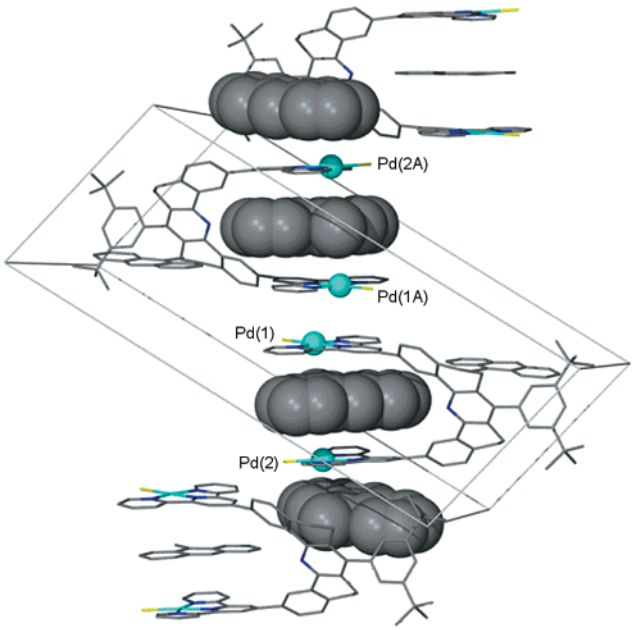

Figure 5. An illustration of the extended structure of [(**16**)Pd_2Cl_2-(9-MA)]$^{2+}$•9-MA. The box is the unit cell, 9-MA molecules of the stack are shown as space-filling models, and the terpy−Pd−Cl units are shown as stick models, as are all other molecules not involved in this stack. Palladium atoms in the stack are shown as blue spheres.

chloride (100 mL), and saturated aqueous $NaHCO_3$ (25 mL) was added. This was stirred for 5 min. The layers were separated, and the organic layer was washed again with saturated $NaHCO_3$ (1 × 10 mL) followed by brine (1 × 25 mL). The organic layer was collected and was dried over $MgSO_4$. Filtration followed by removal of the solvent yielded 5.6 g of the crude product. This was chromatographed on 60 g of basic alumina using 1:1/tetrahydrofuran:hexanes as the eluent. The collected product was then crystallized from methylene chloride/hexanes to yield the product as white crystals (5.00 g, 90.1%), mp 148.5 °C. ^{1}H NMR (CD_2Cl_2, 500 MHz): δ 2.21 (m, 2H), 2.71 (t, J = 6.09, 2H), 3.07 (t, J = 5.99, 2H), 7.38 (m, 2H), 7.47 (d, J = 7.99, 1H), 7.90 (m, 2H), 8.04 (dd, J_1 = 2.13, J_2 = 5.82, 1H), 8.51 (d, J = 2.07, 1H), 8.68 (m, 2H), 8.73 (m, 2H), 8.80 (s, 2H). ^{13}C NMR (CD_2Cl_2, 100 MHz): δ 23.55 29.85, 39.48, 118.74, 121.40, 124.28, 125.74, 130.11, 133.50, 137.17, 145.90, 149.30, 149.53, 156.31, 156.45, 198.02. Anal. Calcd for $C_{25}H_{19}N_3O$: C, 79.55; H, 5.07; N, 11.13. Found: C, 79.85; H, 4.78; N, 11.39.

2-(3,5-Di-*tert*-butyl-benzylidene)-7-[2,2′;6′,2″]terpyridin-4′-yl-3,4-dihydro-2H-naphthalen-1-one (24). A 200 mL flask was charged with the tetralone, **23**, (1.80 g, 4.77 mmol) and 3,5-di-*tert*-butyl-benzaldehyde (1.56 g, 7.15 mmol). This was dissolved in warm tetrahydrofuran (10.8 mL), and to this colorless solution was slowly added a 4 wt % solution of KOH in methanol (48 mL). The color of the reaction mixture became green and then quickly faded to yellow. After 2 h of stirring, the product began to precipitate as a nearly white powder. The reaction was stirred for 36 h at room temperature. During this time the color of the solution continued to lighten, and more of the product precipitated. The reaction was then diluted with methanol (40 mL) and was cooled to −15 °C. Filtration afforded the crude product, which was washed with methanol followed by pentane. The crude product was crystallized from methylene chloride and hexanes to yield the product as white needles (2.00 g, 72.5%). ^{1}H NMR (CD_2Cl_2, 400 MHz): δ 1.37 (s, 18H), 3.06 (m, 2H), 3.23 (m, 2H), 7.36 (d, J = 1.38, 2H), 7.39(m, 2H), 7.47 (m, 2H), 7.89−7.94 (m, 3H), 8.06 (dd, J_1 = 2.10, J_2 = 5.79, 1H), 8.61 (d, J = 2.01, 1H), 8.70 (m, 2H), 8.74 (m, 2H), 8.83 (s, 2H). ^{13}C NMR (CD_2Cl_2, 100 MHz): δ 27.60, 29.09, 31.51, 35.14, 118.82, 121.43, 126.36, 124.29, 124.72, 126.81, 129.52, 131.92, 134.47, 135.15, 135.34, 137.20, 137.55, 138.27, 144.65, 149.46, 149.56, 151.32, 156.35, 156.48, 187.70. Anal. Calcd for $C_{40}H_{39}N_3O$: C, 83.15; H, 6.80; N, 7.27. Found: C, 83.21; H, 6.72; N, 7.34.

7-(3,5-Di-*tert*-butyl-phenyl)-2,12-bis-[2,2′;6′,2″]terpyridin-4′-yl-5,6,8,9-tetrahydro-dibenzo[*c*,*h*]acridine (16). A 500 mL flask was flame dried under a continuous stream of argon. The flask was charged with **24** (3.20 g, 5.54 mmol) and the tetralone, **23**, (1.49 g, 3.96 mmol). These solids were thoroughly mixed before BF_3•Et_2O (10.5 mL) was added to form a yellow-colored mixture. The reaction was then slowly heated to 115 °C (using an oil bath) and was maintained at this temperature for 8 h. During this time all of the starting materials dissolved, the color darkened to brown, and near the end of the time, the product began to precipitate. The reaction material was permitted to cool to room temperature and was dissolved in methylene chloride (50 mL) and methanol (5 mL). This bright yellow solution of the crude pyrylium ion was cooled to 0 °C. To this was carefully added an ammonia−methanol solution (260 mL, 2.0 M, 0.520 mol). This was then permitted to slowly warm to room temperature and was stirred for 48 h. During this time, the color changed from red to a pale yellow. The solvent was then removed under reduced pressure, and the residue was slurried in methanol (15 mL) and was filtered. The crude solid was collected and was washed with methanol (10 mL), ether (10 mL), and pentane (5 mL). This solid was then chromatographed through 125 g of basic alumina using 1:1 tetrahydrofuran:hexanes as the eluant (R_f = 0.5). The appropriate fractions were collected, and the solvent was removed under reduced pressure. The resulting solid was then slurried in ether and was filtered. The ether filtrate was discarded, and the solid was dissolved in methylene chloride and was crystallized by the addition of hexanes. The crystals were collected by filtration, were washed with ether and pentane, and were recrystallized to yield the product as small white crystals (1.80 g, 34.8%), mp > 300 °C. ^{1}H NMR (CD_2Cl_2, 400 MHz): δ 1.41 (s, 18H), 2.67 (broad m, 4H), 2.85 (broad m, 4H), 7.12−7.16 (m, 6H), 7.33 (broad d, J = 7.92, 2H), 7.52 (t, J = 1.74, 1H), 7.74 (m, 4H), 7.82 (d, J = 7.18, 2H), 8.34 (broad s, 4H), 8.47 (d, J = 7.88, 4H), 8.83 (s, 4H), 9.14 (d, J = 1.85, 2H). ^{13}C NMR (CD_2Cl_2, 100 MHz): δ 26.29, 28.27, 31.67, 35.27, 118.93, 121.00, 121.69, 123.51, 123.80, 124.61, 127.47, 128.41, 136.36, 136.74, 137.07, 137.42, 139.38, 149.28, 150.15, 150.34, 151.32, 155.19, 156.01, 156.39. Anal. Calcd for $C_{65}H_{55}N_7$: C, 83.57; H, 5.93; N, 10.50. Found: C, 83.78; H, 6.25; N, 10.13.

7-(3,5-Di-*tert*-butyl-phenyl)-2,12-bis-[2,2′;6′,2″]terpyridin-4′-yl-dibenzo[*c*,*h*]acridine (17). A 25 mL flask was equipped with a condenser was flame dried under a continuous stream of argon. The flask was charged with **16** (0.200 g, 0. 214 mmol) dissolved in hot, anhydrous 1,4-dioxane (13 mL). To the hot solution was added 2,3-dichloro-5,6-dicyano-1,4-benzoquinone (DDQ) (0.486 g, 2.14 mmol). Upon addition, the color of the reaction immediately became brown-red. The reaction was then refluxed. During the first hour of reflux, the color changed to a brown-yellow, and precipitated solids were observed. The reaction was refluxed for a period of 26 h with periodic sonication to break up the precipitate. The reaction was poured into 50 mL of a saturated Na_2CO_3 solution. This was warmed to 65 °C and was stirred at this temperature for 1 h with periodic sonication. The precipitated product was collected by filtration and was washed with distilled water (100 mL). The slightly colored solid was dissolved in 50 mL of CH_2Cl_2 and was washed with saturated $NaHCO_3$ (25 mL), distilled water (25 mL), and brine (25 mL). The organic layer was collected and was dried over Na_2SO_4. Filtration, followed by removal of the solvent afforded the crude product as a tan-colored solid. This was dissolved in tetrahydrofuran and was chromatographed using basic alumina (10 g) with tetrahydrofuran as the eluent. The appropriate fractions were combined, and the solvent was removed under reduced pressure. The yellow-colored solid was then dissolved in methylene chloride (4 mL) and was crystallized by the addition of ether to afford pale yellow needles (0.185 g, 93.0%), mp > 300 °C. ^{1}H NMR (CD_2Cl_2, 500 MHz): δ 1.58 (s, 18H), 7.20 (m, 4H), 7.35 (s, 2H), 7.70−7.86 (m, 9H), 8.14 (d, J = 7.91, 2H), 8.31 (d, J = 0.89, 4H), 8.36 (d, J = 7.72, 2H), 8.46 (d, J = 7.93, 4H), 9.13 (s, 4H), 10.58 (s, 2H). ^{13}C NMR (CD_2Cl_2, 100 MHz): δ 31.87, 35.47, 118.36, 120.94, 123.72, 123.94, 125.09, 126.41, 128.84, 127.16, 127.45, 127.86, 131.76, 131.76, 133.28, 136.84, 137.33, 144.85, 145.09, 149.20, 151.47, 151.83, 156.21. Anal. Calcd for $C_{65}H_{51}N_7$: C, 83.93; H,5.53; N, 10.54. Found: C, 83.73; H, 5.35; N, 10.52.

Tetrakis(acetonitrile)palladium(II) Hexafluorophosphate. A 100

mL flask was flame dried under a continuous stream of argon. Anhydrous acetonitrile (23 mL) was placed in the flask and was degassed for 20 min by bubbling argon through the liquid. Then palladium sponge (0.200 g 1.88 mmol) and nitrosonium hexafluorophosphate (0.704 g, 4.02 mmol) were added, forming a pale green-colored solution. The mixture was heated to 60 °C using an oil bath and was maintained at this temperature for 4 h. During this time, the color changed to yellow, and a steady evolution of NO gas was observed. After this time, a small amount of palladium sponge remained, and the evolution of NO had ceased. The reaction was filtered under argon through a dried Schlenk filter. To the yellow solution was then added 50 mL of anhydrous ether dropwise which resulted in the crystallization of the product. The mixture was then Schlenk filtered again under argon to collect the product as nearly white crystals. The crystals were washed with anhydrous ether (15 mL) followed by pentane (5 mL) and were dried under vacuum. The white crystals are somewhat moisture-sensitive, decomposing over a period of several hours in the air (0.95 g, 90%). The complex was stored under argon at −25 °C. ^{1}H NMR (CD_3NO_2, 500 MHz): δ 2.65 (s). ^{13}C NMR (CD_3NO_2, 125 MHz): δ 3.75, 126.12. Anal. Calcd for $C_8H_{12}F_{12}N_4P_2Pd$: C, 17.14; H, 2.16; N, 9.99. Found: C, 16.96; H, 2.18; N, 9.98.

[(16)Pd$_2$(CH$_3$CN)$_2$](PF$_6$)$_4$. A 10 mL flask was flame dried under a continuous stream of argon. The flask was charged with tetrakis-(acetonitrile)palladium(II) hexafluorophosphate (0.0600 g, 0.108 mmol) which was dissolved in anhydrous acetonitrile (4 mL), forming a pale yellow solution. To this was added the ligand, **16**, (0.0500 g 0.0535 mmol) as a solid. The ligand rapidly dissolved, and the color changed to an orange-yellow. The reaction was stirred at room temperature for 5 h, during which time the color lightened. The reaction was then vapor-diffused with ether, causing the product to precipitate as a yellow powder. The product was collected by filtration and was washed with ether (10 mL), followed by pentane (5 mL) (0.928 g, 95.9%). Many of the ^{1}H NMR signals for this complex remain broad even when the temperature is elevated to 57 °C or the solution is diluted. ^{1}H NMR (CD_3CN, 500 MHz): δ 1.38 (s, 18H), 1.96 (s, 6H), 2.80 (t, J = 7.25, 4H), 3.06 (t, J = 7.07, 4H), 7.15 (d br, 2H), 7.60 (t, J = 1.68, 1H), 7.63 (d, J = 7.96, 2H), 7.95 (br, 4H), 8.02 (br d, J = 7.18, 4H), 8.32−8.40 (br m, 6H), 8.50−8.17 (br m, 8H), 9.32 (br d, J = 1.85, 2H). Λ_M = 334 Ω^{-1} cm^2 mol^{-1}. Anal. Calcd for $C_{69}H_{61}F_{24}N_9P_4Pd_2$: C, 45.81; H, 3.40; N, 6.97. Found: C, 46.10; H, 3.64; N, 6.91.

[(17)Pd$_2$(CH$_3$CN)$_2$](PF$_6$)$_4$. A 10 mL flask was flame dried under a continuous stream of argon. The flask was charged with tetrakis-(acetonitrile)palladium(II) hexafluorophosphate (0.0603 g, 0.108 mmol) which was dissolved in anhydrous acetonitrile (4 mL), forming a pale yellow solution. To this was added the fully oxidized ligand, **17**, (0.0500 g 0.0538 mmol) as a solid. The ligand dissolved during the first minutes of reaction, and the color became light yellow. The reaction was stirred at room temperature for 4 h, after which time the reaction solution was vapor-diffused with ether, causing the product to crystallize as small yellow needles. The crystals were collected and were washed with ether (10 mL), followed by pentane (10 mL) (0.092 g, 95%). ^{1}H NMR (CD_3CN, 400 MHz): δ 1.44 (s, 18H), 1.96 (s, 6H), 7.46 (d, J = 1.80, 2H), 7.80 (t, J = 1.80, 1H), 7.82 (d, J = 9.25, 2H), 7.95−8.04, (m, 6H), 8.36 (d, J = 8.33, 2H), 8.43−8.49 (m, 10H), 8.56 (d, J = 3.82, 4H), 8.88 (s, 4H), 10.67 (d, J = 1.76, 2H). Λ_M = 384 Ω^{-1} cm^2 mol^{-1}. Anal. Calcd for $C_{69}H_{57}F_{24}N_9P_4Pd_2$: C, 45.91; H, 3.18; N, 6.98. Found: C, 45.96; H, 3.04; N, 6.83

[(16)Pd$_2$Cl$_2$](PF$_6$)$_2$. In a 50 mL flask, [(**16**)Pd$_2$(CH$_3$CN)$_2$](PF$_6$)$_4$ (0.181 g, 0.100 mmol) was dissolved in acetonitrile (12 mL), forming an orange-yellow solution of the complex. To this was added, dropwise, tetraethylammonium chloride (0.0332 g 0.200 mmol) dissolved in methanol (2 mL). Upon addition of the chloride, the color of the solution lightened to a pale yellow. The reaction was stirred at room temperature for 1 h. The solvent was then removed under reduced pressure to yield a yellow powder. This was slurried in methanol (10 mL) and was filtered; the solid was washed with excess methanol followed by ether (10 mL) and pentane (10 mL). The yellow solid was dissolved in a minimum amount of hot acetone and was vapor-diffused with ether to yield small yellow crystals (0.146 g, 96.7%). ^{1}H NMR (CD_3CN, 500 MHz): δ 1.47 (s, 18H), 2.97 (t, J = 7.24, 4H), 3.12 (t, J = 7.15, 4H), 7.29 (d, J = 1.76, 2H), 7.31 (br, 4H), 7.68 (d, J = 7.71, 2H), 7.73 (t, J = 1.75, 1H), 7.88 (dd, J_1 = 1.97, J_2 = 7.64, 2H), 8.01 (t, J = 7.36, 4H), 8.06 (br, 4H), 8.14 (d, J = 7.81, 4H), 8.44 (s, 4H), 9.00 (d, J = 1.93, 2H). Λ_M = 235 Ω^{-1} cm^2 mol^{-1}. Anal. Calcd for $C_{65}H_{55}Cl_2F_{12}N_7P_2Pd_2$: C, 51.78; H, 3.68; N, 6.50. Found: C, 51.39; H, 3.48; N, 6.81.

Molecular Rectangle formed with [(16)Pd$_2$(CH$_3$CN)$_2$](PF$_6$)$_2$ and 4,4′-Dipyridyl. A 50 mL flask was charged with [(**16**)Pd$_2$(CH$_3$CN)$_2$](PF$_6$)$_2$ (0.194 g, 0.107 mmol) dissolved in acetonitrile (20 mL), forming a yellow solution. To this was added 4,4′-dipyridyl (0.0168 g, 0.107 mmol) as a solid, in one portion. Upon addition, the intensity of the yellow color lightened slightly. The reaction was stirred at room temperature for 1 h, and the solvent was removed under reduced pressure to leave a yellow powder. This was slurried in 10:1 pentane: acetone (11 mL) and was filtered. The powder was washed with methanol (5 mL) tetrahydrofuran (5 mL), ether (5 mL), and pentane (2.5 mL) (0.188 g, 98.4%). The ^{1}H NMR spectrum of the molecular rectangle is highly symmetrical. Both the spacer-chelators and the 4,4′-dipyridyl groups of the rectangle have identical chemical shifts consistent with a D_{2h} point group on the NMR time scale. ^{1}H NMR (CD_3CN, 500 MHz): δ 1.40 (s, 36H), 2.80 (t, J = 7.08, 8H), 3.08 (t, J = 7.09, 8H), 7.18 (d, J = 1.75, 4H), 7.59 (d, J = 4.69, 8H), 7.61 (t, J = 1.78, 2H), 7.68−7.71 (m, 12H), 8.06 (dd, J_1 = 2.06, J_2 = 6.66, 4H), 8.38 (d, J = 6.57, 8H), 8.42 (td, J_1 = 1.37, J_2 = 8.86, 8H), 8.47 (d, J = 7.75, 8H), 8.76 (s, 8H), 9.28 (d, J = 6.44, 8H), 9.43 (d, J = 1.97, 4H). Λ_M = 527 Ω^{-1} cm^2 mol^{-1}. Anal. Calcd for $C_{150}H_{126}F_{48}N_{18}P_8Pd_4$: C, 47.84; H, 3.37; N, 6.69. Found: C, 47.99; H, 3.36; N, 6.80. ESI-MS: a series of peaks were observed consistent with [M-*n*-(PF$_6$)]$^{n+}$·*m*(CH$_3$CN) (n = 1−7, m = 0,2): for example, 1110.3 [M-3(PF$_6$)]$^{3+}$.

Molecular Rectangle formed with [(17)Pd$_2$(CH$_3$CN)$_2$](PF$_6$)$_2$ and 4,4′-Dipyridyl. [(**17**)Pd$_2$(CH$_3$CN)$_2$](PF$_6$)$_2$ (0.0500 g, 0.02770 mmol) was dissolved in acetonitrile (10 mL) in a 25 mL flask, forming a yellow solution. To this solution was added 4,4′-dipyridyl (0.00433 g, 0.0277 mmol) in one portion, as a solid. The dipyridyl rapidly dissolved, and the intensity of the color lightened somewhat. The reaction was stirred at room temperature for 1 h. Half of the acetonitrile was removed in vacuo, and the solution was vapor-diffused with ether to yield the product as small yellow needles (0.0481 g, 92.3%). The ^{1}H NMR spectrum of the molecular rectangle is highly symmetrical. Both the spacer-chelators and the 4,4′-dipyridyl groups of the rectangle have identical chemical shifts consistent with a D_{2h} point group on the NMR time scale. ^{1}H NMR (CD_3CN, 500 MHz): δ 1.50 (s, 36H), 7.54 (d, J = 1.74, 4H), 7.78−7.82 (m, 16H), 7.90 (t, J = 1.72, 2H), 7.94 (d, J = 9.15, 4H), 8.05 (d, J = 9.32, 4H), 8.42 (d, J = 8.25, 4H), 8.48 (dd, J_1 = 1.81, J_2 = 7.67, 4H), 8.54−8.59 (m, 16H), 8.65 (d, J = 7.73, 8H), 9.10 (s, 8H), 9.49 (d, J = 6.34, 8H), 10.57 (d, J = 1.94, 4H). Λ_M = 511 Ω^{-1} cm^2 mol^{-1}. Anal. Calcd for $C_{150}H_{118}F_{48}N_{18}P_8Pd_4$: C, 47.94; H, 3.16; N, 6.71. Found: C, 47.23; H, 3.13; N, 6.76. ESI-MS: a series of peaks were observed consistent with [M-*n*(PF$_6$)]$^{n+}$·*m*(CH$_3$CN) (n = 1−7, m = 0,2): for example, 402.4 [M-7(PF$_6$) +2(CH$_3$CN)].

Bis(8-hydroxyquinolinato)palladium(II) (27). Palladium(II) acetate (0.112 g, 0.499 mmol) was dissolved in tetrahydrofuran (5 mL) and was filtered through Celite into a 25 mL flask. The resulting solution was concentrated under vacuum to a volume of 5 mL. 8-Hydroxyquinoline (0.145 g, 1.03 mmol) was dissolved in tetrahydrofuran (2 mL) and was added dropwise to the stirred solution of the acetate. Upon addition of the ligand, the color of the solution gradually lightened. After 2 min of stirring, the product began to precipitate as fine, yellow-orange crystals. The reaction was stirred for 15 min. Then, triethylamine (140 μL, 1.00 mmol) was added to the reaction mixture. The reaction was stirred for 10 min. The reaction was then cooled to 0 °C and was filtered. The crystals were washed with cold tetrahydrofuran (5 mL), methanol (5 mL), ether (5 mL), and pentane (5 mL). The crystals were then dissolved in nearly boiling dimethylformamide (35 mL) and filtered. Upon cooling, the product deposited as lustrous, orange blades. The crystals were collected by filtration and were washed with 10 mL each of methanol, ether, and pentane (0.140 g, 71.1%). ^{1}H NMR (CD_2Cl_2, 400 MHz): δ 6.97 (dd, J_1 = 0.89, J_2 = 7.92, 2H), 7.02 (dd, J_1 = 0.79, J_2 = 8.03, 2H), 7.42−7.48 (m, 4H), 8.33 (dd, J_1 = 1.37, J_2 = 8.45, 2H), 8.48 (dd, J_1 = 1.39, J_2 = 4.89, 4H). Anal. Calcd for $C_{18}H_{12}N_2O_2Pd_2$: C, 54.77; H, 3.06; N, 7.10. Found: C, 54.68; H, 2.83; N, 7.15.

Chloro(2,2′,2″-terpyridine)palladium(II) Hexafluorophosphate (25). A 25 mL flask was charged with tetrakis(acetonitrile)palladium(II) hexafluorophosphate (0.150 g, 0.268 mmol) dissolved in dry acetonitrile (13 mL). To this pale yellow-colored solution was added [2,2′;6′,2″]terpyridine (0.0624 g, 0.268 mmol) as a solid. The terpyridine dissolved within 1 min, and the color lightened to pale yellow; soon after, the product began to precipitate as a fine yellow powder. The reaction was stirred at room temperature for 30 min, and the solvent was removed in vacuo. The product was slurried in a 2:1 ether: acetonitrile (6 mL) solution and was filtered. The product was then washed with ether followed by pentane. This yielded 0.168 g of the acetonitrile complex. The acetonitrile complex was dissolved in warm acetonitrile (25 mL), and to this faintly colored solution was added tetraethylammonium chloride (0.0415 g, 0.250 mmol) in methanol (3 mL). Upon addition, the color changed to nearly colorless. After about 2 min, the product begins to precipitate as a nearly white solid. The reaction was stirred for 30 min, and the solvent was removed under reduced pressure. The resulting solid was slurried in methanol. This slurry was filtered and the powder washed with methanol, ether, and pentane. This yields the product as a nearly white powder (0.123 g, 94.6%). ^{1}H NMR (CD_3NO_2, 400 MHz): δ 7.76 (m, 2H), 8.30−8.39 (m, 6H), 8.51 (t, $J = 7.78$, 1 H), 8.69 (dd, $J_1 = 0.78$, $J_2 = 5.47$, 2H). ^{13}C NMR (CD_3NO_2, 100 MHz): δ 125.45, 126.23, 130.09, 143.87, 144.31, 153.81, 156.48, 159.44.

Host−Guest Interaction of [(16)Pd$_2$Cl$_2$](PF$_6$)$_2$ with 9-Methylanthracene. The procedure described here will serve to illustrate the methods used for all host−guest complexation studies. A series of 5.00 mM solutions of [(**16**)Pd$_2$(Cl)$_2$](PF$_6$)$_2$ in CD_3CN containing varying amounts of 9-methylanthracene, ranging from 0.5 to 50 mM, were prepared. The solutions were permitted to equilibrate for at least 2 h before they were examined by ^{1}H NMR and spectrometry. The host alone is yellow in color, and the guest alone is nearly colorless. The host/guest mixtures varied from slightly golden at low concentrations of guest to orange-red at high concentrations of guest. The maximum chemical shift change for any proton of the host was 0.28 ppm. Several other protons of the host had maximum changes of approximately 0.2 ppm. The maximum chemical shift change observed for the guest was 0.35 ppm, with several other chemical shifts changing by about 0.2 ppm. The spectrometry results do not obey Beer's law. The stoichiometry was determined by the "mole ratio" method to be two guest molecules per one host molecule, by plotting the change in chemical shift versus the mole ratio of guest to host for several protons of each.[30] The 2:1 stoichiometry was also suggested by examining the spectrometry data. Equilibrium constants were determined using a modification of the algorithm developed by Anslyn.[31] The assumption is made that the system is in a stepwise equilibrium, eqs 2 and 3

$$H + G \overset{K_1}{\rightleftharpoons} HG \tag{2}$$

$$H + G \overset{K_2}{\rightleftharpoons} HG_2 \tag{3}$$

where H is the host, G is the guest, HG is the host with one guest complex, HG_2 is the host with two guests complex, K_1 is the association constant for one guest with the host, and K_2 is the association constant for the host−guest complex with another guest.

Initial estimates of K_1 and K_2 in conjunction with the goal-seeking function in EXCEL were used to find the real root of eq 4

$$K_1K_2[G]^3 + K_1(2K_2[H]_o - K_2[G]_o + 1)[G]^2 + (K_1[H]_o - K_1[G]_o + 1)[G] - [G]_o = 0 \tag{4}$$

where [G] is the concentration of free guest in solution, $[H]_o$ is the total concentration of the receptor, and $[G]_o$ is the total concentration of guest. Using the determined value of [G] and the initial estimates for K_1 and K_2, the values of [HG] and $[HG_2]$ could be calculated using eqs 5 and 6, respectively.

$$[HG] = (K_1[H]_o[G])/(K_1K_2[G]^2 + K_1[G] + 1) \tag{5}$$

$$[HG_2] = (K_1K_2[H]_o[G]^2)/(K_1K_2[G^2] + K_1[G] + 1) \tag{6}$$

From a mass balance and the values determined for [HG], and $[HG_2]$, the concentration of free receptor, [H], can be determined using eq 7.

$$[H] = [H]_o - [HG] - [HG_2] \tag{7}$$

Knowing the values for $[G]_o$ and $[H]_o$, and employing the calculated values for [H], [HG], and $[HG_2]$ determined for the estimated K_1 and K_2, a predicted chemical shift for the host protons can be calculated using eq 8

$$\delta_{host} = ([H]\delta_H + [HG]\delta_{HG} + [HG_2]\delta_{HG2})/([H]_o) \tag{8}$$

where δ_H is the known chemical shift of a proton of the free receptor, δ_{HG} is the estimated value of the chemical shift for a proton of the receptor as a 1:1 complex, and δ_{HG2} is the observed saturation value of the host proton chemical shift. The predicted values of the chemical shifts for several protons were then compared to the observed values by calculating the sum of the squares of the differences between the actual and predicted data. The values for K_1, K_2, and δ_{HG} were systematically varied and the minimum error was determined. This procedure yielded values of $K_1 = 650 \pm 50$ M^{-1} and $K_2 = 200 \pm 50$ M^{-1}.

Host−Guest Interaction of [(16)Pd$_2$Cl$_2$](PF$_6$)$_2$ with Bis(8-hydroxyquinolinato)palladium(II). Due to the low solubility of the bis(8-hydroxyquinolinato)palladium(II) in the absence of the host, solutions of the guest molecule could not be prepared as before. Rather, into several vials were placed varying amounts of bis(8-hydroxyquinolinato)-palladium(II), and to these were added the solutions of the host. For this series of complexation reactions, the concentration of the host was maintained at 2.74 mM, and the concentration of the guest was varied between 0.253 and 4.66 mM. The color of the host alone is yellow, as is the color of the guest alone. Upon mixing, the color of the solutions varied from slightly orange at low concentrations of the guest to red at the highest concentrations of the guest. For all solutions up to and including the 1:1 mixture, the guest molecule completely dissolves. However, for solutions containing more than 1 equiv of the guest, the bis(8-quinolinato)palladium(II) did not completely dissolve even with prolonged warming. The maximum change in the chemical shift observed for the host was 0.49 ppm. Several other shifts of the host were approximately 0.4 ppm. The maximum chemical shift change observed for the guest was 0.66 ppm. Several other protons of the guest had chemical shift changes of about 0.45 ppm.

Crystallographic Structural Determination for [(16)Pd$_2$Cl$_2$](PF$_6$)$_2$·(9-MA)$_2$·(CH$_3$CN)$_{1.5}$. X-ray quality crystals of the complex were grown by dissolving a 1:2 mixture of [(**16**)Pd$_2$Cl$_2$](PF$_6$)$_2$:9-methylanthracene in acetonitrile and vapor-diffusing with methanol. The orange needles that resulted effluoresce, and thus they were stored in the mother liquor.

A suitable crystal was selected and fastened to a thin glass fiber using silicone grease. A preliminary unit-cell determination was obtained by harvesting reflections from three orthogonal sets of 15 frames, using −0.3° ω scans. These results were confirmed by refinement of unit-cell parameters during integration. Crystallographic information is summarized in Table 1. The structure was solved using direct methods. Non-hydrogen atoms were located by difference Fourier synthesis and were refined anisotropically. Hydrogen atoms were added at calculated positions and treated as isotropic contributions with thermal parameters defined as 1.2 or 1.5 times that of the parent atom. All software and sources of scattering factors are contained in SHELXTL program library (version 5.10, G. Sheldrick, Bruker-AXS, Madison, WI.).

The *E*-statistics for [(**16**)Pd$_2$Cl$_2$](PF$_6$)$_2$·(9-MA)$_2$·(CH$_3$CN)$_{1.5}$ suggested a centrosymmetric space group. The adduct, which was treated as centrosymmetric at all stages of data processing, cocrystallized with three molecules of acetonitrile in the unit cell. A difference map from early in the refinement process located linear chains of electron density that suggested the presence of disordered acetonitrile; the refinement of atoms at these positions did not improve the overall quality of the structure. Squeeze/Platon[35] was applied to account for the electron density associated with solvent in the lattice. Within the 885.3 Å^3 void

space occupied by solvent molecules, a total of 123 electrons was calculated, compared to 146 electrons predicted for the presence of three molecules of acetonitrile. In this treatment, the contribution of the solvent molecules is collective and not as individual atoms. Hence, the atom list does not contain the atoms of the solvent molecules.

The small crystal size and diffuse diffraction data, attributed to the apparent solvent loss, made it necessary to constrain the rings of the 9-methylanthracene molecules to planar hexagons with C−C distances of 1.394 Å. Further restraints were also needed to prevent gross deformation of one *tert*-butyl group on the ligand. Nevertheless, refinement of atoms at the core of the host molecule proceeded smoothly.

(35) PLATON, Spek, A. L. *Acta Crystallogr*. **1990**, *A46*, C34.

Acknowledgment. This work was supported by grants from the Department of Energy.

Supporting Information Available: Tables of crystal data, atomic coordinates and equivalent isotropic displacement parameters, bond lengths and angles, anisotropic displacement parameters, and hydrogen coordinates and isotropic displacement parameters for [(**16**)Pd_2Cl_2]$(PF_6)_2$·(9-MA)$_2$·$(CH_3CN)_{1.5}$ (PDF). This material is available free of charge via the Internet at http://pubs.acs.org.

JA004279V